Materials Today: Proceedings 35 (2021) 538–541

Contents lists available at ScienceDirect

Materials Today: Proceedings

journal homepage: www.elsevier.com/locate/matpr

Multilayered MoS_2/C nanospheres as high performance additives to lubricating oils

Volodymyr Kotsyubynsky [a], Lyudmyla Shyyko [a], Thaer Shihab [b], Pavlo Prysyazhnyuk [c], Victor Aulin [d], Volodymyra Boichuk [a,*]

[a] Vasyl Stefanyk Precarpathian National University, 57 Shevchenko Str., Ivano-Frankivsk 76018, Ukraine
[b] Middle Technical University/Engineering Technical College-Bagdad, Azafaraniya Main Str., Bagdad 29132, Iraq
[c] Ivano Frankivsk National Technical University of Oil and Gas, 15 Karpatska Str., Ivano-Frankivsk 76018, Ukraine
[d] Ukraine Central Ukrainian National Technical University, 8 Prospekt Universytetskyi Str., Kropyvnytskyi 25006, Ukraine

ARTICLE INFO

Article history:
Received 16 September 2019
Accepted 10 October 2019
Available online 6 November 2019

Keywords:
MoS_2
Carbon
Nanospheres
Composite
Critical point of failure

ABSTRACT

The main goal of the present work was the investigation of tribological properties of multilayered hydrothermally synthesized MoS_2/C nanospheres as an additive to industrial base oil. The average size of the MoS_2/C particles in which MoS_2 layers alternate with carbon is about 40 nm. The tests were performed for reciprocating motion conditions through "plane-ball" scheme. The main tribological characteristics (critical point of failure and friction coefficient) changes as functions of the lubricant additives concentration were discussed. The time dependencies of the tribological characteristic were fitted by sigmoid functions. It was found that the addition of 0.1 wt% MoS_2/C nanoparticles to the base oils results in 30% up in friction coefficient reduction and 10 times enlarging of critical point of failure.

Selection and peer-review under responsibility of the scientific committee of the XVII International Freik Conference on Physics and Technology of Thin Films and Nanosystems.

1. Introduction

Solid lubricants (metal dichalcogenides or carbon based materials) as the additives to oils are intensively investigated for a last decades [1]. Graphite is an classic example of a carbon-based material that has layered structure with a hexagonal lattice (space group 194 P63/mmc) and high c/a ratio (c = 0.670 nm°, a = 0.246 nm) [2] in which carbon atoms in its basal planes are held with strong covalent bonds, while the basal planes themselves are held together by weak Van der Waals cohesive forces, resulting in interplanar mechanical weakness. Thus, it is traditionally thought that under a shearing force the basal planes slide over one another by intracrystalline slip, often referred to as "deckof-cards" shear. Another carbon-based additive, including onion-like carbon [3–5], carbon nanotubes [6], graphene [7,8], nanodiamonds [9] and even carbon blacks [10] have been evaluated in various types of lubricants. Similar to graphite, 2H-MoS_2 (typical layered transition metal sulfide) crystallizes in the hexagonal structure where a sheet of molybdenum atoms is sandwiched between two hexagonally packed sulfur layers. Due to the Van der Waals gaps between MoS_2 layers, they are easy to slide under the friction shearing. In addition, S atoms in MoS_2 have an intensive adsorption effect on the metal surface. These characteristics may provide persistent lubrication for metal friction pairs in extreme environments such as at high temperature and high vacuum [11,12]. On the other hand, on ion-like carbon particles or carbon nanotubes with excellent mechanical characteristics (such as high tensile strength, high elastic modulus) and high thermal and electrical conductivity [6] maintain their concentric graphitic structure even under 1 GPa contact pressure [5], while the spherical nanostructures of MoS_2 or WS_2-type became squashed or fractured under high pressures during the sliding action and eventually transformed into a lubricious planar lamellar tribolayer on the sliding surface in order to reduce friction. Thus, combining carbon with transition metal dichalcogenides relying on their structural similarity allow to obtain new composite with improved properties, such as mechanical strength. Effectiveness of the additives strictly depends on the particle size and morphology [13]. Nano-particles have very high surface area to volume ratio and hence provide very large interfacial area, as a driving force for enhanced interaction with other surface, diffusion, especially at elevated temperature etc. For example,

* Corresponding author.
E-mail address: vmbojchuk@gmail.com (V. Boichuk).

https://doi.org/10.1016/j.matpr.2019.10.021
2214-7853/
Selection and peer-review under responsibility of the scientific committee of the XVII International Freik Conference on Physics and Technology of Thin Films and Nanosystems.

MoS_2 nanosheets could strongly adhere to substrates and get optimized orientations with the next enhancing of the tribological properties [14]. While forming layer-closed structures, such as inorganic fullerene-like, tube-like and hollow sphere-like, may eliminate the active rim-edge surface and increase the chemical stability of nano-MoS_2. It was established that the lowest friction coefficient occurred in the nano-sphere/micro-platelet composite (20 wt% nano-spheres and 80 wt% micro-platelets) [15]. MoS_2 nano-platelets may present the shearing and sliding lubrication mechanism and the excellent tribological properties of spherical nano-MoS_2 may be explained by its chemical inertness, rolling friction, deformation, and exfoliation-delivery of MoS_2 sheets to the contact area. According to [16] the exfoliation of the spherical nanoparticles is the dominant mechanism at the high normal stress. Rolling is an important only in the relatively low range of normal stress and sliding is relevant when the spacing between the two mating surfaces does not permit the nanoparticles size.

In this work we report the tribological testing of spherical and lamellar (as a result of some nanospheres disruption) multilayer nanoparticles with double-hierarchical structure in which MoS_2 layers alternate with carbon.

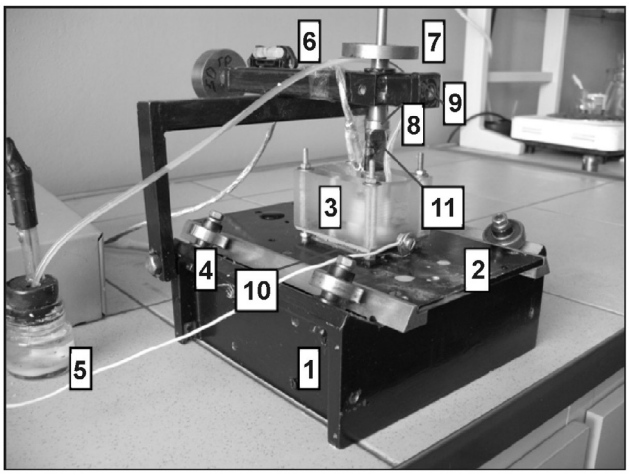

Fig. 2. The equipment for tribological tests in the reciprocating motion conditions (1) – frame; 2 – table; 3 – cell for corrosion protection; 4 – bearings; 5 – Ag-AgCl reference electrode; 6 – water level; 7 – weights system; 8 – indenter; 9 – balance beam; 10 – sample; 11 – strain sensors.

2. Experimental details

Multilayered MoS_2/C nanospheres were obtained by hydrothermal synthesis using cetyltrimethylammonium bromide as a micelle forming agent. Full description of synthesis procedure and materials properties in details is reported in [17] and [18]. The obtained material is a complex of agglomerated particles with nearly spherical shape and dimensions up to 80 nm (Fig. 1, a) with the average size about 40 nm. Double-hierarchical structure in which MoS_2 layers alternate with carbon was observed. The surface layer of particles with the thickness of 10 nm is characterized by crystalline order, and the interior hollow spaces within the particles are partially filled with amorphous material. Shell of spherical particles is composed of 7–9 layers of carbon and S-Mo-S packages (Fig. 1, b).

Morphological characteristics and chemical composition were obtained by TEM and EDS (FEI Technai G2 X-TWIN microscope).

The powder of MoS_2/C after mortar milling have been added to the industrial oil in concentration of 0.015, 0.025 and 0.1 wt% with the next ultrasonic desperation. Tribology tests were carried out using reverse scheme "plane of 40 × 50 mm (composite based on chromium carbide [19]) – the ball of d = 10 mm (corundum Al_2O_3)-". The procedure of tribological investigations of contacting couples in controlled media under the conditions of reversible friction by using a microprobe of lubricants is described in [20] (Fig. 2). An electric motor and a worm gear performed the reciprocating motion of table 2 and are placed on the frame 1. Bearings 4 guaranteeing the rectilinear of motion of table 2 are also installed on the frame. Specimen 10 is placed on the surface of the table 2. This table is attached to bath 3 with screws (through a rubber seal). The sample 10 was placed on the table 2 and has been pressed to steel plane by cell 3 through the rubber gasket. Samples loading was realized by weights system 7 installed on the vertical indenter 8. The balance beam 9 with fixed indenter 8 was exposed horizontally using water level 6. Vertical indenter 8 with strain sensors 11 moves in the vertical direction in the rocker. The design of the laboratory setup allows determining antifriction characteristics

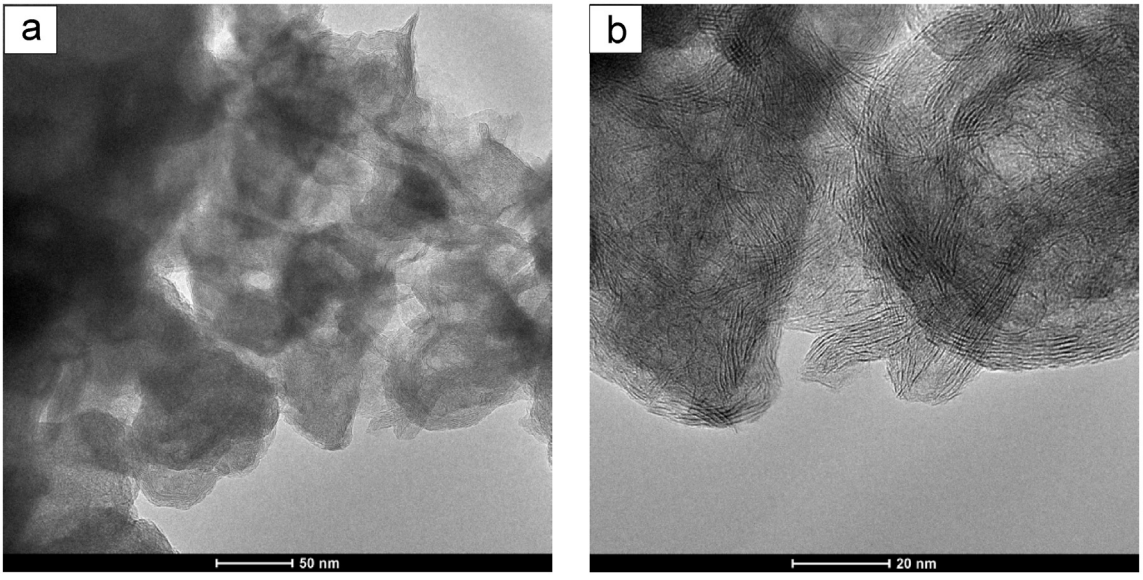

Fig. 1. TEM images of the material obtained by hydrothermal synthesis.

for a wide range of lubricants in ceramic – metal, ceramic– cermet [21] and ceramic – composite coating [22].

The conditions of tribological tests: the period of the cycle and total test duration were 4 s and 3500 s respectively. Maximum Hertzian contact pressure was 0.9 GPa. Average integral values of friction coefficient per one cycle were determined.

3. Results and discussion

Friction coefficient changes with test time for pure oil and prepared mixes are presented on Fig. 3. The interaction of pure lubricant oil with friction surface leads to the formation of semicrystalline boundary layers perceiving the external loads. During mutual movement of the friction surfaces the distortion shift of semicrystalline layers occurs that reduces the friction force in comparison with the friction without lubricant. Mechanical interaction between microscopic roughnesses of the contact surfaces causes formation of the adhesive bonds, destruction of the boundary layers and increasing of the local temperature. Both normal and shear stresses and also enlarged temperature lead to mechanical degradation of lubrication layer and significant changes of the surface energy of oil due to redistribution its consistuens [23]. As a result load-carrying capacity of boundary layer decreases that results in friction coefficient sharp growth from 0.16 to 0.28 (mark *cpf1* on the Fig. 3).

The destruction of antifriction protective boundary layer at the reverse motion is accompanied by the formation of the surface tracks (scratches) and leads to friction coefficient sharp increasing with its next stabilization on the relatively higher level. According to obtained chart (Fig. 3) the increasing of additive content causes the non-linear decreasing of new "stabilized" values. At the same time the duration of transitions to this state non-linearly increases. Due to the fitting results, the changes of the friction coefficients (μ) versus test time (t) were optimally approximated by sigmoid functions (coefficients of determination for all cases were less 0.90):

$$\mu = \mu_2 + \frac{\mu_1 - \mu_2}{1 + e^{\frac{(t-t_0)}{\sigma}}} \quad (1)$$

with μ_1 and μ_2 are "stabilized" values of friction coefficients before and after the antifriction layer destruction, respectively; t_0 is a time moment when the friction increase is the highest, σ is a parameter which characterizes the transition time.

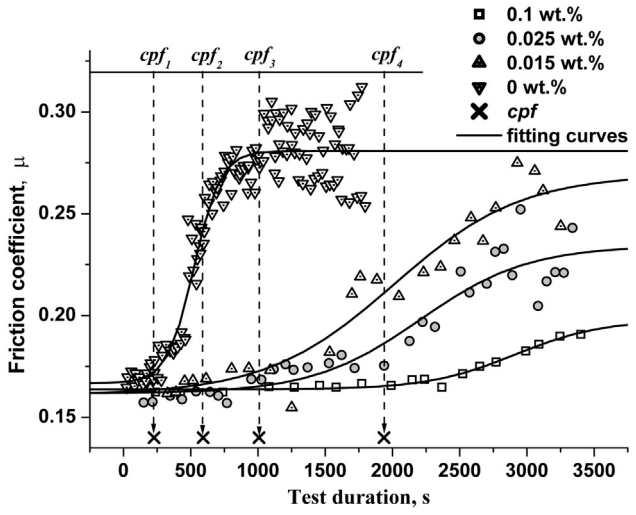

Fig. 3. Friction coefficient versus time for pure oil and oil with MoS2/C additives in concentration 0.015, 0.025 and 0.1 wt%. Lines represent the fitted results by Eq. (1).

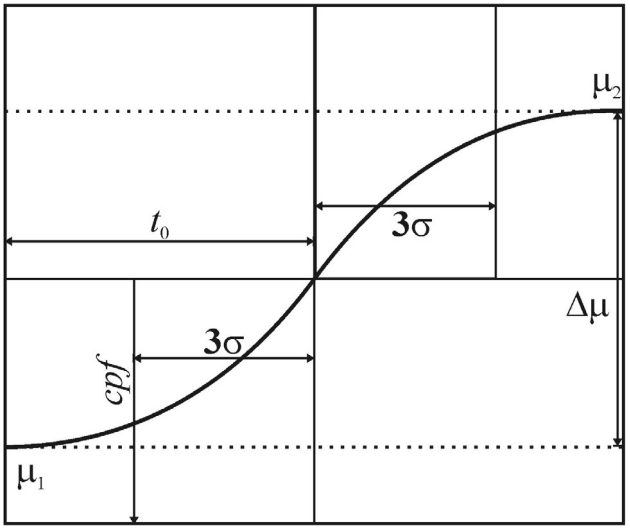

Fig. 4. Critical point of failure (*cpf*) determination scheme.

One of the most important criteria of antifriction additives effectiveness at reciprocation is the starting time of friction coefficient growth – critical point of failure (*cpf*) [24]. For cpf determination three-sigma rule of normal distribution was used:

$$cpf = t_0 - 3\sigma \quad (2)$$

As a result, *cpf* is a moment of time before the friction coefficient growing by 10% (Fig. 4).

Another important parameter which characterizes the efficiency of lubricantadditives is the value of the friction coefficient jump (K_μ) after reaching cpf during a period of time with duration of 6σ [25]. Parameter K_μ was determined as $K_\mu = \mu_1/\mu_2$ (at $K_\mu = 1$ the destruction of lubricating film does not occur) [26].

The obtained dependences of tribotechnical parameters cpf and K_μ as functions of MoS_2/C additives concentration (Fig. 5) were fitted by sigmoid functions (coefficients of determination are close to 0.99):

$$cpf(c) = cpf_{\min} + (cpf_{\max} - cpf_{\min})\frac{c^n}{k^n + c^n} \quad (3)$$

$$K_\mu(c) = K_{\mu\min} + (K_{\mu\max} - K_{\mu\min})\frac{c^n}{k^n + c^n} \quad (4)$$

with *cpf* min, $K_{\mu min}$ are minimum and cpf_{max}, $K_{\mu max}$ are maximum (asymptotic) values of *cpf* and K_μ, respectively; k is a concentration of additive at which the tribotechnical characteristic equals half the sum of the maximum and minimum values, n is a constant.

Parameters K_μ and cpf increased sharply with the concentration enlarging from 0.015 to 0.025 wt% (Fig. 5). At the same time further increasing of the additive concentrations had no significant effect on K_μ and cpf. As a result, the optimal content of MoS_2 / C additive at which the critical point of failure increases in 10 times is about 0.1 wt%. This concentration of additives is 3–5 times lower than the typical values of microcrystal molybdenum disulphide concentration in lubricating oil.

4. Conclusion

The effectiveness of multilayered hydrothermally synthesized MoS_2/C nanospheres as an oils additive was investigated. Tests were performed using the reverse "plane - ball" scheme. Time dependencies of the friction coefficient for different MoS_2/C additives concentrations were analyzed using of sigmoid fitting

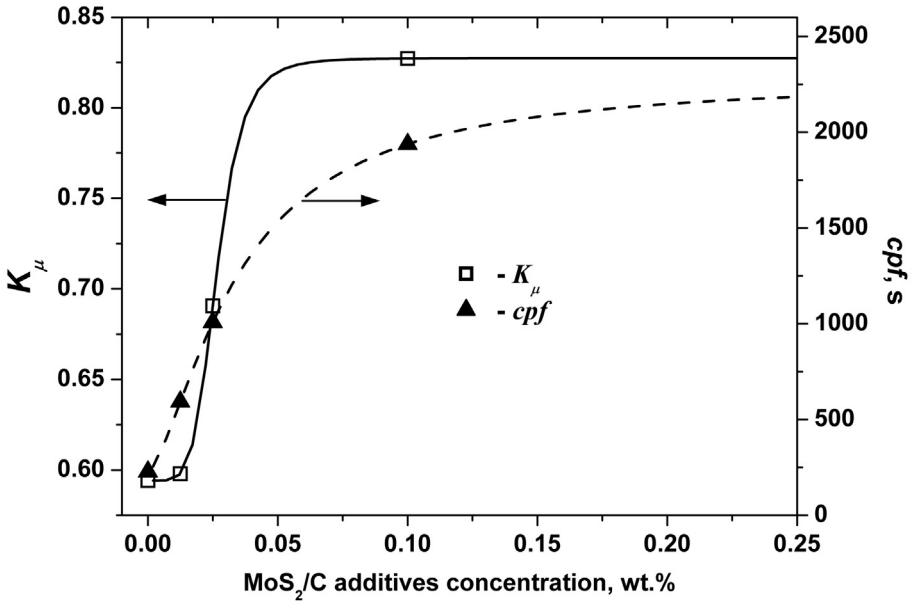

Fig. 5. Tribotechnical characteristic cpf and Kμ versus MoS2/C additives concentration. Lines represent the fitted results by Eqs. (2) and (3), respectively.

function. It was determined that the enlarging of MoS_2 /C additives in industrial base oil up to 0.1 wt% causes the friction coefficient decreasing from 0.281 to 0.198 and critical point of failure grew about 10 times. Tested additives contents are about 3–5 times lower than the typical values of microcrystal molybdenum disulphide concentration in industrial oils at the condition of similar tribological properties.

References

[1] T. Spalvins, J. Vac. Sci. Technol. 5 (2) (1987) 212–219.
[2] P. Delhaes, Graphite and Precursors. World of carbon, 1st ed., Gordon and Breach Science Publishers, Amsterdam, 2000.
[3] N. Ohmae, J. Tribol. Int. 39 (12) (2006) 1497–1502.
[4] L. Joly-Pottuz, B. Vacher, N. Ohmae, J.M. Martin, Tribol. Lett. 30 (1) (2008) 69–80.
[5] N. Matsumoto, L. Joly-Pottuz, H. Kinoshita, N. Ohmae, Diam. Relat. Mater. 16 (7) (2007) 1227–1230.
[6] H. Liu, H. Ji, H. Hong, Y. Hammad, Ind. Lubr. Tribol. 66 (5) (2014) 579–583.
[7] D. Berman, A. Erdemir, A.V. Sumant, Carbon 59 (2013) 167–175.
[8] D. Berman, A. Erdemir, A.V. Sumant, Carbon 54 (2013) 454–459.
[9] V.N. Mochalin, O. Shenderova, D. Ho, Y. Gogotsi, Nat. Nanotechnol. 7 (2011) 11–23.
[10] S. Baik, D. Yoon, H.I. Lee, J.M. Kim, G.S. Lee, Y.Z. Lee, Tribol. T. 52 (1) (2008) 133–137.
[11] Z. Zhang, W. Liu, Q. Xue, J. Zen, J. Tribol. 18 (4) (1998) 377–382.
[12] C.G. Dunckle, M. Aggleton, J. Glassman, P. Taborek, J. Tribol. Int. 44 (2011) 1819–1826.
[13] X. Hu, Ind. Lubr. Tribol. 57 (6) (2005) 255–259.
[14] Z. Wu, D. Wang, Y. Ohmae, A. Sun, Adv. Eng. Mater. 12 (6) (2010) 534–538.
[15] K.H. Hu, Y.K. Cai, X.G. Hu, Y.F. Xu, Ind. Lubr. Tribol. 65 (3) (2013) 143–149.
[16] O. Tevet, P. Von-Huth, R. Popovitz-Biro, R. Rosentsveig, H.D. Wagner, R. Tenne, Proc. Natl. Acad. Sci. 108 (50) (2011) 19901–19906.
[17] L. Shyyko, V. Kotsyubynsky, I. Budzulyak, M. Rawski, Y. Kulyk, R. Lisovski, Phys. Status Solidi A 212 (10) (2015) 2309–2314.
[18] L.O. Shyyko, V.O. Kotsyubynsky, I.M. Budzulyak, P. Sagan, Nanoscale Res. Lett. 11 (1) (2016) 243.
[19] P.M. Prysyazhnyuk, T.A. Shihab, V.H. Panchuk, Mat. Sci. 52 (2) (2016) 188–193.
[20] V.A. Vynar, V.M. Dovhunyk, M.M. Student, Mat. Sci. 46 (5) (2011) 633–639.
[21] Ya.A. Kryl, P.M. Prysyazhnyuk, J. Superhard Mater. 35 (5) (2013) 292–297.
[22] D.L. Lutsak, P. Prysyazhnyuk, M. Karpash, V. Pylypiv, V. Kotsyubynsky, Metallofiz. Noveishie Tekhnol. 38 (9) (2016) 1265–1278.
[23] P. Prysyazhnyuk, D. Lutsak, A. Vasylyk, S. Thaer, M. Burda, Metall. Min. Ind. 12 (2015) 346–350.
[24] M.S. Won, O.V. Penkov, D.E. Kim, Carbon 54 (2013) 472–481.
[25] V. Aulin, O. Lyashuk, O. Pavlenko, D. Velykodnyi, A. Hrynkiv, S. Lysenko, D. Holub, Y. Vovk, V. Dzyura, M. Sokol, Commun.-Sci. Lett. Univ. Zilina 21 (2) (2019) 3–12.
[26] V. Aulin, A. Hrynkiv, S. Lysenko, I. Rohovskii, M. Chernovol, O. Lyashuk, T. Zamota, Eastern-Eur. J. Enterp. Technol. 1 (97) (2019) 6–12.